This article has been accepted for publication in a future proceedings of this conference, but has not been fully edited. Content may change prior to final publication. Citation information: DOI: 10.1109/upec65436.2025.11279846, 2025 60th International Universities Power Engineering Conference (UPEC)

Design and Implementation of a Resonant Inductive Wireless Charging System for Electric Vehicles Compliant with SAE J2954

Bektur Ogobaev
Brunel University of London, UK
2017975@brunel.ac.uk

Muhammad Salman Sikandar
Engineering School (ENGME),
Uxbridge College, UK
Salman.Sikandar@hruc.ac.uk

Muhammad Shaikh
Engineering School (ENGME),
Uxbridge College, UK
Muhammad.shaikh@hruc.ac.uk

Mohamed Darwish
Brunel University of London, UK
mohamed.darwish@brunel.ac.uk

***Abstract*—The main objective of the paper is to present design, simulation and implementation of a wireless charging system (WCS) for electric vehicles (EVs) based on resonant inductive coupling. The system operates at 85 kHz to comply with SAE J2954 standard while employing Series-Series (SS) compensation topology. Simulated efficiency of the system is 86% at resonance with a coupling coefficient factor of 0.3. A scaled down prototype further validates the wireless power transfer (WPT) principle.**

I. Introduction

WPT is the transference of power from transmitter to receiver without the need for electrical wires or connections. It operates through magnetic or electric fields across an air gap and commonly employs principles of electromagnetic induction and resonance. In terms of application WPT has a wide range of uses, starting from smaller consumer-based products such as toothbrush and phone chargers to bigger applications such as automation for electrical vehicle charging and more.

As the adoption of cleaner energy increases the importance of EVs rises in multiple magnitudes. Thus, it plays a key role in the future automotive industry due to the higher mass adoption driven by multiple causes such as lesser gas emissions and overall reduction in pollution. Additionally, they bring the benefit of user convenience and automation. Wireless Charging Systems also completely ignore wear and tear, which is usually caused by the wired systems. Plus, the potential of dynamic wireless charging, which enables EVs to charge while on the move [1].

The study focuses on design, simulation and physical implementation of a static WCS for EVs. The system uses the resonant inductive coupling methodology while incorporating a SS compensation topology. Lastly, to comply with SAE J2954 standard the system operates at 85 kHz resonant frequency [2]. The main objective is to evaluate the system's efficiency and feasibility through simulation and practical approaches. Thus, laying the groundwork for scalable WPT applications for EVs.

II. Related Work

This paper will focus on investigating and developing a WCS with a resonant inductive coupling WPT method. This choice is based on a comparison of all WPT methods, such as capacitive, inductive, microwave, and radiofrequency WPT. The resonant inductive coupling possesses the best mid-range power transfer capability and higher tolerance towards coil misalignment. This is the result of both primary and secondary sides being tuned to the same operating resonant frequency, ultimately, creating a strong magnetic flux linkage between primary and secondary sides.

Additionally, the system will employ an SS compensation network because it provides the most optimized power transfer performance. Due to the topology possessing load-independent current characteristics on the primary side plus stability under different loads. This makes it ideal for EV charging applications. Furthermore, the system will comply with the SAE J2954 standard which requires WCS to operate at 85 kHz due to Electromagnetic Interference (EMI), balancing between component size and efficiency etc. [3].

III. System Design

The block diagram (Figure 1) represents the overall design and order of logic which the WCS follows. Consisting of three major dashed block sections which are primary (blue box), secondary (blue box) and wireless power transfer (orange box). Thus, closely following a typical design of a standard WCS.

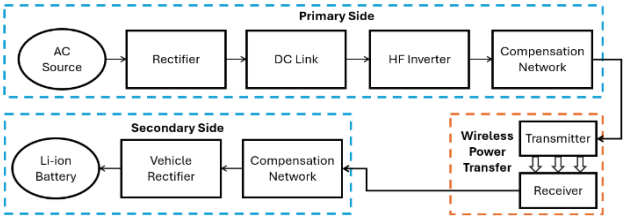

Figure 1: Block diagram representation of the WCS

In this scenario the diagram starts with the AC source which outputs 230V and 50Hz. The corresponding voltage is then rectified, thus converting AC voltage into DC. Next, due to power undergoing multiple conversions on the primary side of the system (Figure 1). A DC link is placed between the source rectifier and the High Frequency (HF) inverter in order to provide some stabilization.

Afterwards, the stabilized DC voltage is then converted into high frequency AC with the use of the HF Inverter. Thus, achieving the desired 85kHz for the WPT as SAE J2954 standard states that this frequency is the balance between efficiency, electromagnetic compatibility and interoperability across different manufacturers [4]. The high frequency AC

then goes through the primary compensation network towards the transmitter coils. At this step due to the WPT the power is transferred inductively towards the receiver coil. The wirelessly transferred high frequency AC then goes through the secondary side compensation network towards the vehicle rectifier. This specific step is crucial as the lithium-ion (Li-ion) battery is a DC component. As a result, the system ultimately charges the battery.

Table 1: Considered list of components for the WCS's

Component	Specification
Power Supply	230V, 50Hz (AC)
Rectifier	Diodes: D1, D2, D3, D4.
DC Link	DC link: Capacitor in parallel DC link: Inductor in series
HF Inverter	Pulse Width Modulation (PWM) DC-DC control for 85kHz IGBT/Diodes Switches: S1, S2, S3, S4.
Compensation Network	Series to Series Compensation Network: Capacitor in series
Transmitter & Receiver coils	Primary Winding: Inductor Secondary Winding: Inductor
Li-ion battery	Nominal voltage: 360V Rated capacity: 100Ah Battery Capacity: 36kWh

A. Justification and operation of chosen components

First, as previously mentioned in the requirements section the 230V 50Hz AC supply was chosen due to the intention of designing the system for a home use. Specifically, regulating to the UK's standard mains electricity supply voltage.

Second, before proceeding to the DC link and the HF inverter the AC needs to be rectified. This is accomplished by employing four diodes in a bridge configuration in order to be able to conduct the full AC wave and rectify it into DC.

Third, the DC-link filter serves a crucial role of acting as a filter between the source rectifier and the HF inverter. Thus, requiring the smoothening of the DC voltage and current due to the presence of heavy power conversion (AC to DC) on the primary side of the system. In this case, the filter will be made out of two components the inductor in series and capacitor in parallel. Effectively, filtering voltage ripples with the deployed capacitor and limiting the rate of change of current with the inductor. This ultimately helps to minimize potential high switching losses which could've occurred if unfiltered voltage and current have gone through the HF inverter. Thus, effectively improving the overall power quality by supplying the HF inverter with clean DC power.

Fourth, due to the requirement of AC signal for WPT the employment of an inverter is essential. Thus, creating the needed magnetic field in later stages of the design due to the alternating current in the inductor windings. Additionally, this AC signal has to operate at higher frequency ranges in order to avoid magnetic losses and bulkier design/components (e.g. bigger capacitor and inductor). Thus, in this case four H-bridge IGBT/diode general switches were employed along with the PWM in order to introduce a control mechanism. The AC signal is essentially created due to the PWM operating at 50% duty cycle, thus generating a constant on/off signal. The output of PWM is then split into two directions and one of them will be operating with a NOT gate. This ultimately produces the correct conditions required for the AC generation, as two general switches e.g. S1 and S4 will be on and S2 and S3 will be off then polar opposite will occur and this cycle will keep repeating to generate the required AC shown in Figure 2.

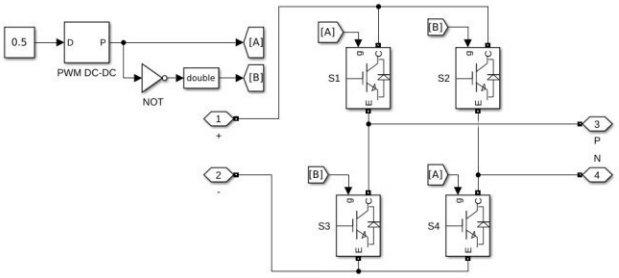

Figure 2: Contraction of HF Inverter with Switches S1,S2,S3&S4

Fifth, SS compensation network is the most suitable for an EV WPT application. Due to its characteristics such as the load independent current in the primary side. Effectively, resulting the transmitter to operate at a fixed power level which improves the overall system stability. Thus, making it ideal for EVs where the load is relatively constant. Additionally, In Table 2 list of topologies has mentioned where the SS compensation network has the best misalignment tolerance out of the 4 topologies which are Series-Parallel (SP), Parallel-Series (PS) and Parallel-Parallel (PP). The other topologies were not chosen due to their specific limitations. Such as: SP requiring high input voltage because of the parallel capacitor on its secondary side, plus its load dependent behavior makes it quite not ideal for EVs. PS in the other hand needs a high frequency current source due to the primary capacitor being in parallel, on top of that at higher frequencies PS topology has a high voltage gain as well. Lastly, PP has high current draw due to both capacitors being in parallel. Making highly inefficient at higher power levels.

Table 2: List of Topologies

1	Series-Series (SS)
2	Series-Parallel (SP)
3	Parallel-Series (PS)
4	Parallel-Parallel (PP)

Lastly, when designing and choosing the right transmitter/receiver windings and the battery type. There are only two optimal choices for this system. First, being the Lithium-ion batteries which simply complement the WPT system due to fast charging capabilities and overall high efficiency. Second, is the benefit of using Litz wires for high frequency applications as it introduces better management of heat and lower losses. Thus, noticeably further enhancing the system's performance.

B. Essential WPT design calculations

There are two essential WPT calculations which need to be kept in mind when designing a WCS. First, is the calculation of capacitor values for the compensation network as shown in Equation 1. As both frequency and inductor values will be preset as desired. In this case, frequency will be tuned to

85kHz for the reasons mentioned before in the requirements section and inductor value will be dictated by the chosen coil configuration. Thus, for theoretical/simulation a value of $160\mu H$ was chosen. The physical implementation will replicate this number through a circular coil design which will also be explored in detail at later stages of the paper. Ultimately, granting the capacitor value of $22nF$ as seen from Equation 2).

Completing this calculation is crucial as it will represent the capacitive value at which both inductive and capacitive reactance cancel each other out. Resulting in minimal losses scenario where a maximum energy exchange between the inductor and capacitor occur. Thus, when incorporating this method and tuning both transmitter and receiver to the same natural frequency a magnetic resonance coupling is achieved. As ultimately both primary and secondary sides start to exchange energy with minimalistic losses. This also eliminates potential reactive power circulation, enabling maximum real power transfer towards the load.

$$C = \frac{1}{(2\pi f)^2 L} \tag{1}$$

$$C = \frac{1}{(2\pi \times 85{,}000)^2 \times 160 \times 10^{-6}} \approx 22nF \tag{2}$$

Second calculation represents the strength of magnetic coupling between the primary and secondary inductor windings as show in Equation 3. It is usually denoted as coupling coefficient (k) and ranging from k=1 for perfect coupling and k<1 for weaker coupling. In realistic scenarios for WPT EV applications with SS compensation network this value ranges from 0.1 to 0.3. Thus, considering this factor is quite crucial as it will influence WPT's power transfer capability, alignment tolerance and overall efficiency,ultimately, figuring out how much magnetic flux from the primary coil is linked to the secondary coil can help to define the mutual inductance value (M). In this case, the most common value for (k) would be 0.3. Thus, granting the mutual inductance of $48\mu H$ as seen from Equation 5.

$$k = \frac{M}{\sqrt{L_1 L_2}} \tag{3}$$

$$0.3 = \frac{M}{\sqrt{160 \times 10^{-6} \times 160 \times 10^{-6}}} \tag{4}$$

$$M = \frac{3}{10} \times \sqrt{160 \times 10^{-6} \times 160 \times 10^{-6}} \approx 48\mu H \tag{5}$$

IV. Simulation

The WCS system created in Matlab is direct implementation of the proposed system design into Simulink simulation (Figure 3). Thus, following the same order of design logic as demonstrated and explained in system design section. First, it starts off with the AC source which outputs 230V and 50Hz (Figure 4). As this a single-phase AC output a Universal Bridge block which has two bridge armed diodes was used. Thus, providing a rectified DC to the DC link series inductor and parallel capacitor, effectively making the DC link have an expected output of 200V and 13A (Figure 5).

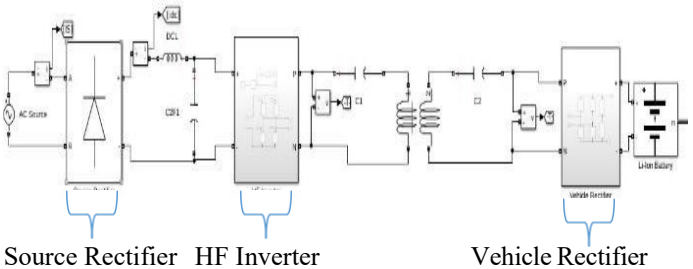

Figure 3: Design of the circuit in Simulink

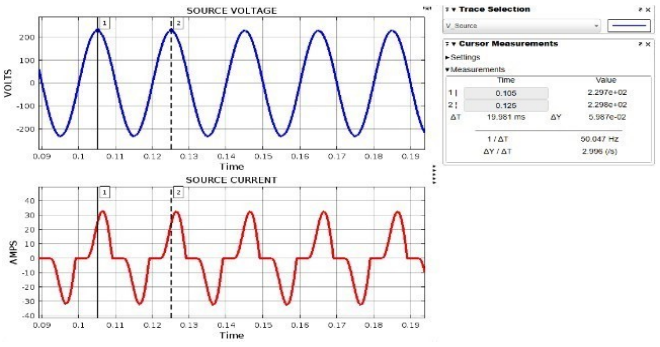

Figure 4: AC source output

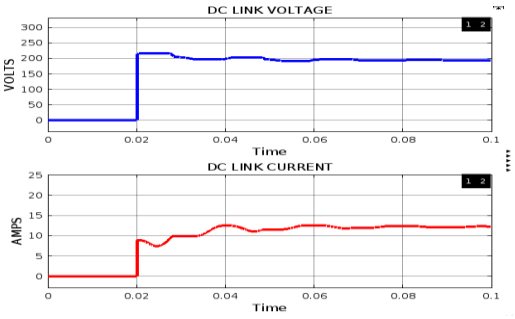

Figure 5: DC Link output

Afterwards, the stabilized DC is then put through the HF inverter in order to raise the frequency to 85kHz and change the power back to AC. This is achieved by constructing a H bridge with 4 different switches which S1 & S4 complement the control signal A and S2 & S3 complement the control signal B.

These two complementary signals (A&B) are then driven one at a time in order to ensure no overlapping of signal is occurring. This is accomplished by: first, setting a 0.5 constant block to PWM frequency generation then second including a NOT block to the control block B. Ultimately, driving only one diagonal pair at a time. Lastly, the frequency is simply set by inputting the desired value into the PWM block. The output is as expected from a HF inverter due to the conversion of DC to AC through means like switches resulting in a square wave output instead of sinusoidal. Thus, roughly outputting AC voltage of 290V and 19A (Figure 6). Also, most importantly the output frequency has changed as desired from 50 Hz to 85 kHz.

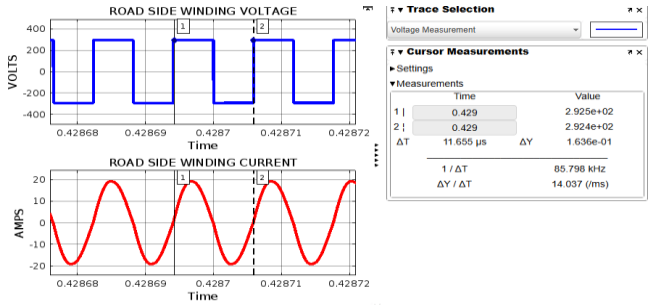

Figure 6: Roadside winding/HF Inverter output

After the HF Inverter the signal passes through the primary SS Compensation Network capacitor which has a value of $22nF$. Then, to the primary windings at which WPT occurs towards the secondary windings (both with $160\mu H$ inductors). Thus, due to the WPT the output of voltage is now roughly around 390V and 13A (Figure 7). Eventually, reaching the vehicle rectify by going through the secondary SS Compensation Network capacitor with the similar value of $22nF$. Thus, signifying a 1:1 WPT as both inductor and capacitor values of primary and secondary are identical. Finally, after the vehicle rectification the power is eventually delivered to the Li-ion Battery. Thus, charging the battery from 51.644% to 51.645% in 1 second (Figure 8). Lastly, the mutual inductance commonly denoted with the letter (M) is $48\mu H$ and the coupling coefficient (k) used is 0.3, shown in Table 4.

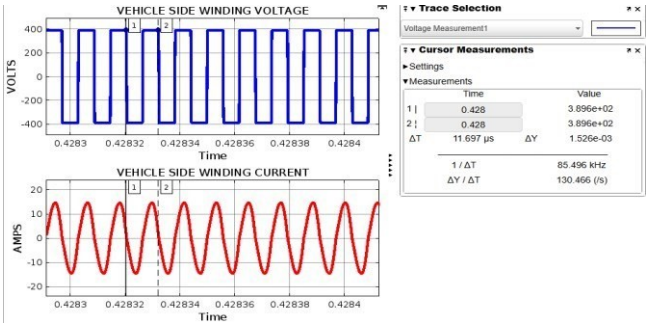

Figure 7: Vehicle Side winding output

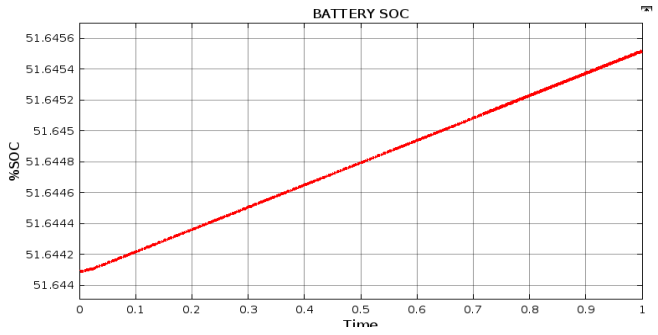

Figure 8: State of charge (SOC) of the battery

A. *Different test conditions*

This section will contain the testing of the simulated circuit under different conditions. Mainly focusing on the WPT aspect of the system. Thus, exploring the importance of frequency matching magnetic resonance and influences of misalignment on the coupling coefficient factor of the system.

1) *Frequency matching*

The main objective of this test is to verify that the system is tuned to the right resonance frequency by manipulating the frequency value generated by the PWM. Therefore, multiple tests at different frequency ranges will be carried out. 2 of them being within the plausible range of ±5 kHz (80 kHz and 90kHz). The rest of the two tests will be carried out in extremely different frequency ranges e.g. ± 55 kHz. (30 kHz and 140kHz).

Table 3: Efficiency of the system at different range of frequencies

Frequency	Efficiency
85 kHz	86%
80 kHz	78%
90 kHz	82%
30 kHz	-2.5%
140 kHz	-2.5%

As expected, the efficiency of the WCS is at its highest when tuned to its resonance frequency which is 85 kHz (Table 3). This is simply since compensation network and windings were specifically configured to operate at this frequency. Thus, even slightly changing the operating frequency through PWM it had an instant impact on the overall efficiency of the system. Suggesting poorer flux linkage between primary and secondary windings. This fact is even more evident when observing extreme frequency changes such as 30 kHz and 140 kHz. As they both landed on roughly negative 2.5% efficiency.

In a more in-depth analysis, it can be noted that 90 kHz change compared to 80 kHz has higher efficiency. This could be simply due to the system preferring higher frequencies because of its high frequency operating components such as MOSFET etc. Therefore, if switching frequency goes down it will evidently experience higher losses. To counter this, the whole design of the system will need a remastering.

2) *Coupling coefficient factor*

The main purpose of this test is to understand how misalignment can affect the mutual inductance by varying the coupling coefficient (k). Thus, ultimately affecting the overall power transfer of the system. The following realistic values from k=0.1, 0.3 and 0.5 were used and one extremely unrealistic case of k=1. The coefficient value being 1 is indeed quite unrealistic when it comes to the EV WPT application as some distance between the pad and the vehicle must be expected. Even, 0.5 is quite rare as the usual value for EV application usually ranges from 0.1 to 0.3 (Table 4).

Table 4: Efficiency of the system at different coupling coefficient values

Coupling Coefficient (k)	Mutual Impedance	Efficiency
0.3	$48\mu H$	86%
0.1	$16\mu H$	58%
0.5	$80\mu H$	88%
1	$160\mu H$	94%

The results from (Table 4) clearly demonstrate the impact of coupling coefficient (k) on the system. As the value started dropping from 1 to 0.1 efficiency has significantly reduced. Thus, highlighting the importance of not only resonance frequency matching for the WPT but also correct alignment for a better coupling coefficient. This demonstrates a progressive decrease in efficiency as the primary and secondary windings start to gain distance from each other. Furthermore, distance is not the only factor as line of sight (LOS) is also quite crucial. If an object was placed between the primary and secondary sides, then a decrease in performance must be expected.

V. Physical Implementation

Due to hardware and time constraints certain parts of the design had to be adjusted. For example, instead of PWM the frequency was instead directly supplied from the function generator and then towards the HCF4011BE NAND IC. Thus, replicating the positive and negative square wave ACs for the control signal A and B respectively. Furthermore, the 4 MOSFETs used for switching and the HCF4011BE NAND ICs were all lower frequency operating devices. Therefore, the operating resonance frequency had to be changed from 85kHz to around 1kHz. Granting the new calculation of the capacitor as seen from Equation (6). However, the inductor coil value of each winding remained roughly the same (158.1µH) as seen from Figure 10 .

$$C = \frac{1}{(2\pi \times 1000)^2(159 \times 10^{-6})} = 150\mu F \qquad (6)$$

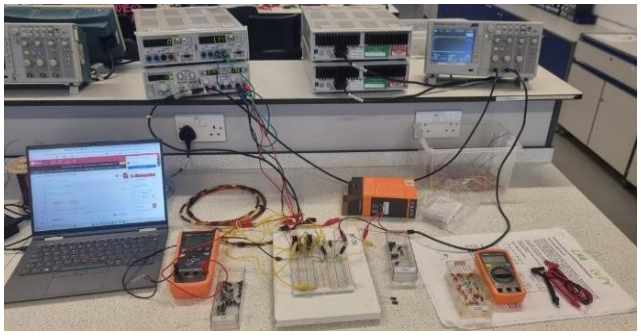

Figure 9: Overall view of the components included in physical implementation

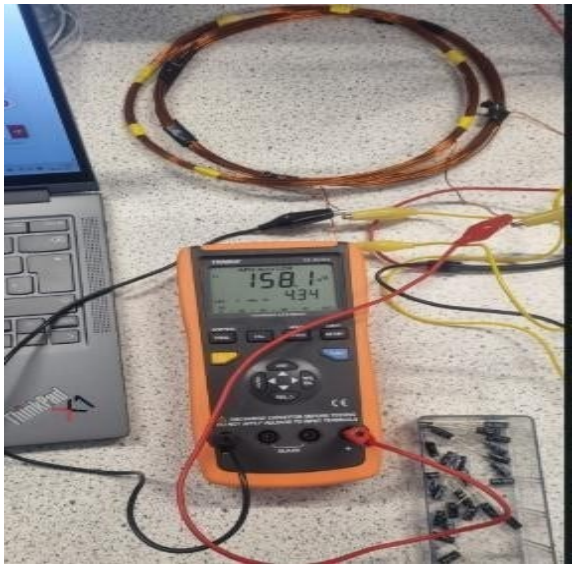

Figure 10: Inductor value of each winding

A. Results

In terms of results, they did not fully match the expected values due to the compromises made in the earlier circuit design section of physical implementation (Figure 11). Specifically referring to the part where instead of PWM a direct feed was used with the NAND IC to replicate a similar input. However, the process of WPT was still indeed occurring as the LED which was set as the load did in fact light up (Figure 12). In the other hand, it is the most likely scenario of 2 opposite square AC signals being cancelled out with each other when being fed towards control signal A and B. As with normal PWM function this would've not happened as it has a step input of 0.5. Thus, each diagonal switch would've had time to turn on and off by taking turns. Also keep in mind that the resonant frequency had to be of low value due to the involvement of low frequency operating components.

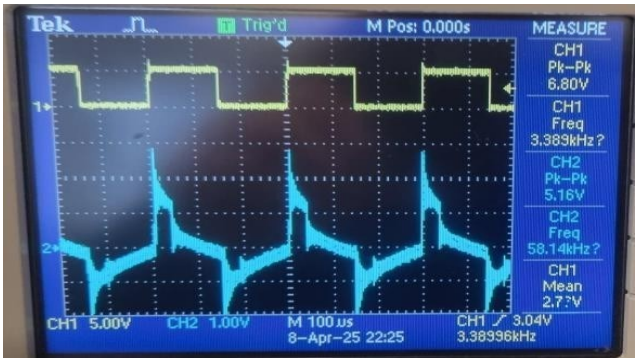

Figure 11: Final output waveform

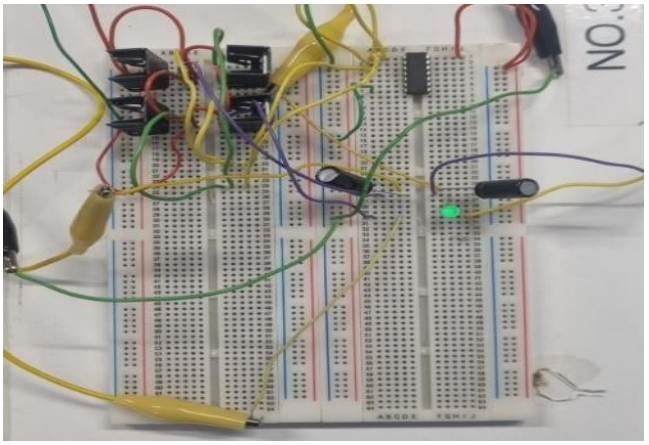

Figure 12: Demonstration of the LED lighting up

Additionally, when trying to operate the circuit at resonant frequency the components started drawing too much current. This was resolved by increasing the frequency to around 3.4 kHz instead. This occurred with any other frequency value as well. Not just with 1 kHz as the output of each in terms of voltage significantly reduced and the system started drawing too much current. The frequency always had to be a few kHz higher than desired.

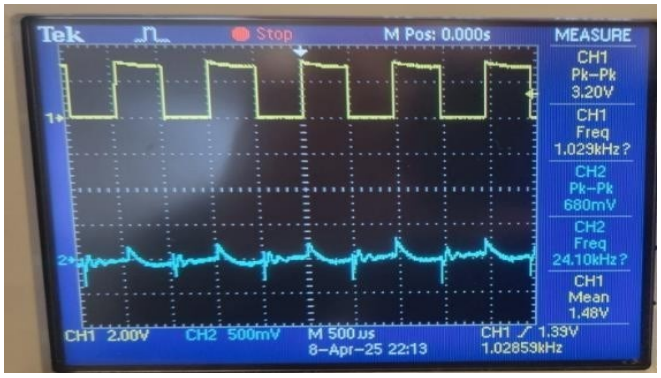

Figure 13: Reduced output at optimal resonance frequency value of 1 kHz

However, it is important to mention that this practical was still useful at proving the simple function of WPT. As with altering distance between the primary and secondary windings and thus changing the coupling coefficient value of (k) the output voltage and current were affected (Table 5). Thus, suggesting a demonstration of successful coil coupling as the magnetic flux linkage between primary and secondary directly controlled the voltage and current output. Furthermore, the validity of WPT as the power was transferred wirelessly through an air gap. Ultimately, demonstrating the elemental function of wireless power transfer. Lastly, all components involved in the physical prototype are listed in (Table 6).

Table 5: Power variance depending on distance between primary and secondary coils

Distance	Voltage	Current
1cm	5.16V	6.2µA
5cm	3.14V	2.2µA
10cm	1.01V	0.1µA

Table 6: List of components

Components	Specification
4 X MOSFET	MTP3055VL
NAND IC	HCF4011BE
Function Generator	1kHz
Power supply	5V 0.5A
Oscilloscope	For measurements
2 X Inductor winding coils	$158.1\mu H$
2 X Compensation capacitors	$150\mu F$

VI. Conclusion and Future Work

In conclusion, the project was successfully designed, simulated and physically implemented by demonstrating a working WPT system for EV charging. Simulation results demonstrated a peak efficiency of 86% at a coupling coefficient of 0.3. Efficiency improved with stronger coupling, confirming the sensitivity of WPT systems to coil alignment. The physical prototype was operated at lower resonant operating frequency due to component and time limitations. However, it still successfully demonstrated wireless energy transfer by successfully illuminating the LED and demonstrating varied voltage and current values as coupling coefficient changed. Thus, validating the core concept of WPT.

Future work will consist of implementation of high frequency operation using suitable MOSFET drivers for physical prototype. Further exploration of WPT towards dynamic charging and incorporation of EMI shielding and other safety mechanisms. Exploring bidirectional power transfer for applications such as Vehicle to Grid etc. Lastly, the implementation of closed loop system with real time feedback from coil alignment sensors to effectively maintain optimal coupling.

References

[1] SimScale, "Wireless Power Transfer: an Overview," *SimScale*, May 14, 2024.https://www.simscale.com/docs/simwiki/electromagnetics/wireless-power-transfer/

[2] SAE International, "J2954_202408: Wireless Power Transfer for Light-Duty Plug-in/Electric Vehicles and Alignment Methodology - SAE International,"*Sae.org*,2024.https://www.sae.org/standards/content/j2954_202408/

[3] SAE Mobilus, "J2954_202010: Wireless Power Transfer for Light-Duty Plug-in/Electric Vehicles and Alignment Methodology - Technical Standard,"*Sae.org*,2020.https://saemobilus.sae.org/standards/j2954_202010-wireless-power-transfer-light-duty-plug-electric-vehicles-alignment-methodology (accessed May 22, 2025).

[4] A. Triviño-Cabrera, J. M. González-González, and J. A. Aguado, *Wireless Power Transfer for Electric Vehicles: Foundations and Design Approach*. Cham: Springer International Publishing, 2020. doi: https://doi.org/10.1007/978-3-030-26706-3.